



www.asianpubs.org

Asian Journal of Materials Chemistry

Volume: 4 Year: 2019
Issue: 1–2 Month: January–June
pp: 18–23
DOI: <https://doi.org/10.14233/ajmc.2019.AJMC-P74>

Received: 14 March 2019

Accepted: 13 May 2019

Published: 29 June 2019

Author affiliations:

Jiangsu Key Laboratory of Green Synthetic Chemistry for Functional Materials, Jiangsu Normal University, Xuzhou 221116, P.R. China

✉ To whom correspondence to be addressed:

Fax: +86 516 83500366
Tel: +86 516 83403165
E-mail: xsp62@jsnu.edu.cn

Available online at: <http://ajmc.asianpubs.org>

ARTICLE

Crystal Structures and Cytotoxicity of Four Silver(I)carboxylate Complexes with 1,2-Ethylenediamine Analogues

Suo-Ping Xu[✉] and Qian Dong

ABSTRACT

Four silver(I) compounds, $[\text{Ag}(\text{dapn})(\text{dnbc})]_n \cdot 1.5n\text{H}_2\text{O}$ (**1**), $[\text{Ag}(\text{en})]_n - [\text{Ag}(\text{dnbc})_2]_n \cdot 2n\text{H}_2\text{O}$ (**2**), $[\text{Ag}(\text{en})]_n [\text{Ag}(\text{nbc})_2]_n \cdot 2n\text{H}_2\text{O}$ (**3**) and $[\text{Ag}(\text{dapn})]_n - (\text{nbc})_n \cdot 2n\text{H}_2\text{O}$ (**4**), where dapn = 1,2-diaminopropane, dnbc = 3,5-dinitrobenzoate, en = 1,2-diaminoethane and nbc = 4-nitrobenzoate, have been synthesized and characterized by X-ray diffraction. The Ag(I) ions show T-shaped coordination geometry in compound **1** but linear coordination geometry in compounds **2**, **3** and **4**. There are ligand-unsupported Ag...Ag interaction in compounds **2** and **3** with Ag...Ag distance of 3.177 ~3.267 Å. All the four complexes showed high cytotoxicity properties.

KEYWORDS

Coordination polymer, Silver compounds, Cytotoxicity.

INTRODUCTION

The coordination chemistry of the coinage metals has been the subject of investigation for decades [1]. Historically, interest in this area grew out of the diverse structural motifs displayed by these superficially similar monovalent cations. More recently, interest has been renewed by practical concerns. Some examples of the concerns promoting research in this area can be listed as follows: such coinage metal complexes can be used as potential precursors to metal films *via* chemical vapor deposition (CVD) processes [2,3]. An alternative method for separating olefins and paraffins is chemical adsorption using silver(I) compounds [4], which form complexes with unsaturated compounds such as olefins and acetylenes but not with saturated compounds such as paraffins [5]. The silver-catalyzed partial oxidation of ethylene to ethylene oxide is one of the most important and thoroughly investigated industrial processes [6–14]. Silver-ethylene and silver-ethylene oxide species are two possible coordination intermediates formed on the silver catalyst surface during the reaction. The complexes of silver(I) with carboxylic acids represent a group of metal compounds which, despite their usage in synthetic organic chemistry [*e.g.*, Hunsdiecker reaction (decarboxylation), Simonini reaction (ester synthesis), and Prevost reaction (diol synthesis)] [15]. Yanagisawa *et al.* [16,17] a catalytic enantioselective aldol addition of tributyltin enolates to aldehydes employing BINAP silver(I) complex as a catalyst (BINAP = 2,2'-bis(diphenylphosphino)-1,1'-binaphthyl). Silver is known to promote the selec-

tive catalytic reduction of nitric oxide by light hydrocarbons over alumina [18-21]. Silver ion can also bind to a large number of sites on a peptide, including the amino nitrogen at the N-terminus, basic groups on the side chain, and the carbonyl oxygens of the peptide bonds [22-24]. Intermolecular addition of an alcohol to alkynes is one of the efficient routes for functionalization of a C-C triple bond [25]. It was reported that some silver compounds showed catalytic activity in the addition of methanol to dimethyl acetylenedicarboxylate (DMAD) [26]. Moreover, the studies of some silver(I) complexes have been mostly related to their antiethylene [27] and antimicrobial activities [28-30]. Silver sulfonamides, particularly silver sulfadiazine [31], have been used as the standard treatment for burns over the past two decades. Silver chloride was assumed to form at the burn wound, and the absorption of silver was believed to be negligible [32]. Silver nylon dressings may be a valuable antimicrobial burn wound covering device [33]. Despite major advances described above, the research on different uses and ideas of various silver(I) compounds is being in the ascendant. The authors are interested in the investigation on silver(I) complexes with various organic ligands containing N and/or O atoms and their cytotoxicity. Thus, the crystal structure of silver(I) carboxylato complexes with ethylenediamine and analogues and its cytotoxicity is discussed.

EXPERIMENTAL

1,2-Diaminopropane (98 %) was purchased from Aldrich and used as received. 1,2-Diaminoethane (97 %), 4-nitrobenzoic acid (98 %) and 3,5-dinitrobenzoic acid (98 %) made in China were used without further purification. All the other reagents and solvents were of A.R. grade specification and used as received. C, H and N elemental analyses were performed on a Perkin-Elmer elemental analyzer.

Preparation of complexes 1-4: $[\text{Ag}(\text{dapn})(\text{dnbc})]_n \cdot 1.5_n \text{H}_2\text{O}$ (**1**), Ag_2O (0.5 mmol, 116 mg) and 3,5-dinitrobenzoic acid (1 mmol, 212 mg) were dissolved in ammonium solution (10 mL), stirring for about 10 min to obtain a clear solution. After standing still the solution in air for 2 days with the ammonia gas escaping large colourless prism crystals were crystallized, isolated, washed with water for three times, and dried in a vacuum desiccator under drying CaCl_2 . In a similar procedure, complexes $[\text{Ag}(\text{en})]_n \cdot [\text{Ag}(\text{dnbc})_2]_n \cdot 2_n \text{H}_2\text{O}$ (**2**), $[\text{Ag}(\text{en})]_n [\text{Ag}(\text{nbc})_2]_n \cdot 2_n \text{H}_2\text{O}$ (**3**) and $[\text{Ag}(\text{dapn})]_n (\text{nbc})_n \cdot 2_n \text{H}_2\text{O}$ (**4**) were obtained. The elemental analysis data for compounds **1** to **4** in Table-1.

X-ray crystallography: Diffraction intensities for silver compounds **1-4** were mounted on a CCD area detector equipped with graphite-monochromated $\text{Mo } K_\alpha$ ($\lambda = 0.71073 \text{ \AA}$) radiation at 293 K using $\omega/2\theta$ scan mode. The final orientation matrices and cell parameters were obtained from least-squares fits. The data sets were corrected for Lorentz-Polarization effect

and a MULTI-SCAN absorption correction was applied using ψ scan techniques. The structure was solved by direct methods, in which heavy-atom positions were revealed. The remaining non-hydrogen atoms were located with use of successive difference Fourier maps and full-matrix least-squares refinement. All the hydrogen atoms were placed in calculated positions and were assigned fixed isotropic thermal parameters at 1.2 times the equivalent isotropic U of the atoms to which they are attached and allowed to ride on their respective parent atoms. The contributions of these hydrogen atoms were included in the structure-factors calculations. All esds (except the esd in the dihedral angle between two l.s. planes) are estimated using the full covariance matrix. The cell esds are taken into account individually in the estimation of esds in distances, angles and torsion angles; correlations between esds in cell parameters are only used when they are defined by crystal symmetry. An approximate (isotropic) treatment of cell esds is used for estimating esds involving l.s. planes. The weighted R-factor wR and goodness of fit S are based on F^2 , conventional R-factors R are based on F, with F set to zero for negative F^2 . The threshold expression of $F^2 > 2\sigma(F^2)$ is used only for calculating R-factors(gt), etc. and is not relevant to the choice of reflections for refinement. R-factors based on F^2 are statistically about twice as large as those based on F and R-factors based on ALL data will be even larger. All calculations were carried on a Bruker SMART computer using SHELXS and SHELXL programs [34]. Crystallographic and experimental data for silver complexes **1-4** are listed in Table-2. Selected bond lengths and angles are reported in Table-3. A CIF table including listings of thermal parameters, bond lengths and angles and hydrogen atom coordinates has been deposited as an accessory publication.

in vitro Cytotoxicity: Five human solid carcinoma cell lines, Hela (cervix adenocarcinoma), HepG2 (hepatocellular carcinoma), BGC (gastric carcinoma), 95-D (lung carcinoma), CNE (rhinocarcinoma) and two normal cell lines, NIH 3T3 (mouse normal fibroblast) and L-02 (human normal liver cell) were obtained from Shanghai Cell Institute of Chinese Science Academy. These cells were subcultured in media RPMI 1640 (GIBCO BRL product) with 10 % fetal bovine serum (hyclone product), at 37 °C with 5 % CO_2 . Cells were adjusted to a concentration of 10^5 cells mL^{-1} and were planted in 96-well tissue culture plate, and were then exposed to the test compounds ranging in concentrations from 2.5 to 100 $\mu\text{g mL}^{-1}$ for 48 h. The cells were pigmented by MTT [3-(4,5-dimethylthiazol-2-yl)-2,5-diphenyltetrazolium bromide] and the O.D. values were measured by ELX800 (universal microplate reader, BIO-TEK Instruments, Inc.) under 490 nm wavelength. The IC_{50} value (concentration of drug required to inhibit 50 % growth) was calculated from linear regression of the percent viable cells versus log of drug concentration (Table-4).

TABLE-1
ELEMENTAL ANALYSIS DATA^a FOR COMPOUNDS **1** TO **4**

Compound	m.f.	C (%)	H (%)	N (%)	Yield (%)
1	$\text{C}_{10}\text{H}_{16}\text{N}_4\text{O}_{7.5}\text{Ag}$	30.01 (29.64)	4.10 (3.98)	39.26 (39.75)	88
2	$\text{C}_{16}\text{H}_{18}\text{N}_6\text{O}_{14}\text{Ag}_2$	26.45 (26.18)	2.55 (2.47)	11.26 (11.45)	73
3	$\text{C}_{16}\text{H}_{16}\text{N}_4\text{O}_8\text{Ag}_2$	31.79 (31.60)	2.77 (2.65)	9.05 (9.21)	71
4	$\text{C}_{10}\text{H}_{18}\text{N}_3\text{O}_6\text{Ag}$	31.36 (31.27)	4.89 (4.72)	10.68 (10.94)	62

^aCalculated values are given in parentheses.

TABLE-2
CRYSTALLOGRAPHIC AND EXPERIMENTAL DATA FOR COMPLEXES 1-4

	Compound 1	Compound 2	Compound 3	Compound 4
Formula	C ₁₀ H ₁₆ AgN ₄ O _{7.5}	C ₁₆ H ₁₈ Ag ₂ N ₆ O ₁₄	C ₁₆ H ₁₆ Ag ₂ N ₄ O ₈	C ₁₀ H ₁₈ AgN ₃ O ₆
FW	420.14	734.10	608.07	384.14
Crystal shape	Long rod	Long needle	Long rod	Rod-like
Crystal size/ mm	0.34 × 0.18 × 0.14	0.26 × 0.13 × 0.08	0.42 × 0.25 × 0.10	0.54 × 0.35 × 0.16
Crystal system	monoclinic	triclinic	triclinic	triclinic
Space group	C2/c	P $\bar{1}$	P $\bar{1}$	P $\bar{1}$
a (Å)	28.123(8)	6.978(2)	6.346(3)	7.139(2)
b (Å)	5.2414(15)	12.919(5)	7.022(3)	7.509(2)
c (Å)	24.723(7)	15.029(5)	23.044(11)	14.007(4)
α (°)	90	84.320(6)	82.638(7)	78.505(5)
β (°)	122.958(4)	76.810(5)	83.169(6)	78.789(4)
γ (°)	90	79.612(6)	67.880(6)	82.023(4)
U (Å ³)	3057.8(15)	1295.2(8)	940.5(8)	717.8(4)
Z	6	2	2	2
T (K)	298(2)	298(2)	298(2)	298(2)
μ /mm ⁻¹ (Mo-K α)	1.022	1.589	2.138	1.432
Dx (g cm ⁻³)	1.369	1.882	2.147	1.777
Reflections (parameters)	3164 (268)	4780 (359)	3696 (335)	2873 (253)
Independent reflections (R _{int})	1904	1816	2916	2353
F(000)	1266	724	596	388
T _{max}	0.8702	0.8834	0.8147	0.8032
T _{min}	0.7227	0.6828	0.4671	0.5118
Goodness of fit on F ²	0.875	0.739	0.964	1.034
R ₁ , wR [I ≥ 2 σ (I)] ^{a)}	0.0365, 0.0621	0.0631, 0.0666	0.0311, 0.0660	0.0361, 0.0916
R ₁ , wR (all data) ^{a)}	0.0691, 0.0700	0.1580, 0.0885	0.0434, 0.0700	0.0452, 0.0960

$R_1 = \Sigma ||F_o| - |F_c|| / \Sigma |F_o|$, $wR_2 = [\Sigma w(F_o^2 - F_c^2)^2 / \Sigma w(F_o^2)^2]^{1/2}$, $w = [\sigma^2(F_o^2) + 0.1(\max(0, F_o^2) + 2F_c^2)/3]^2$ ⁻¹.

TABLE-3
SELECTED BOND LENGTHS (Å) AND
ANGLES (°) FOR COMPLEXES 1-4

Complex 1			
Ag(1)-N(1)	2.169(3)	Ag(1)-O(1)	2.483(3)
Ag(1)-N(2A)	2.194(3)	N(1)-Ag(1)-N(2A)	156.87(14)
N(1)-Ag(1)-O(1)	107.96(12)	N(2A)-Ag(1)-O(1)	91.06(12)
Complex 2			
Ag(1)-N(1)	2.149(5)	Ag(2)-O(3)	2.091(5)
Ag(1)-N(2)	2.168(5)	Ag(2)-O(1)	2.147(5)
Ag(1)-Ag(2)	3.1770(13)	O(3)-Ag(2)-O(1)	174.4(3)
N(1)-Ag(1)-N(2)	175.9(2)		
Complex 3			
Ag(1)-N(3)	2.129(3)	Ag(1)-N(4)	2.130(3)
Ag(2)-O(5)	2.093(3)	Ag(1)-Ag(2)	3.2669(15)
N(3)-Ag(1)-N(4)	178.40(12)	O(5)-Ag(2)-O(1)	178.00(11)
Complex 4			
Ag(1)-N(1)	2.124(3)	Ag(1)-N(2A)	2.132(3)
N(1)-Ag(1)-N(2A)	175.50(12)		

RESULTS AND DISCUSSION

X-ray single crystal diffraction revealed that the compound **1** crystallizes in monoclinic space group C2/c and the asymmetric unit consists of one Ag ions, one 3,5-dinitrobenzoic acid (dnbc), one 1,2-diaminopropane (dapn) and two crystal lattice water molecules (Fig. 1). The Ag(1) ion are coordinated by two nitrogen atoms from two dapn and one carboxylate oxygen from dnbc. The Ag-O bond distance is 2.483(3) and Ag-N distances are 2.169(3) and 2.194(3) Å. The N-Ag-N angle is 156.87(14) and N-Ag-O angles are 107.96(12) and 91.06(12) Å which indicate the coordination geometry of Ag(1) is closer to T- shape rather than triangle. The Ag(1) ions are linked by dapn to form one-dimensional chain as shown in Fig. 1b. The chains are further linked by O-H...O [O(7)...O(7), 2.874; O(7)...O(1), 2.718; O(8)...O(2), 2.952 Å] and C-H...O [C(6)...O(3), 2.730; C(8)...O(4), 2.692 Å] hydrogen bonds results in three-dimensional supramolecular array.

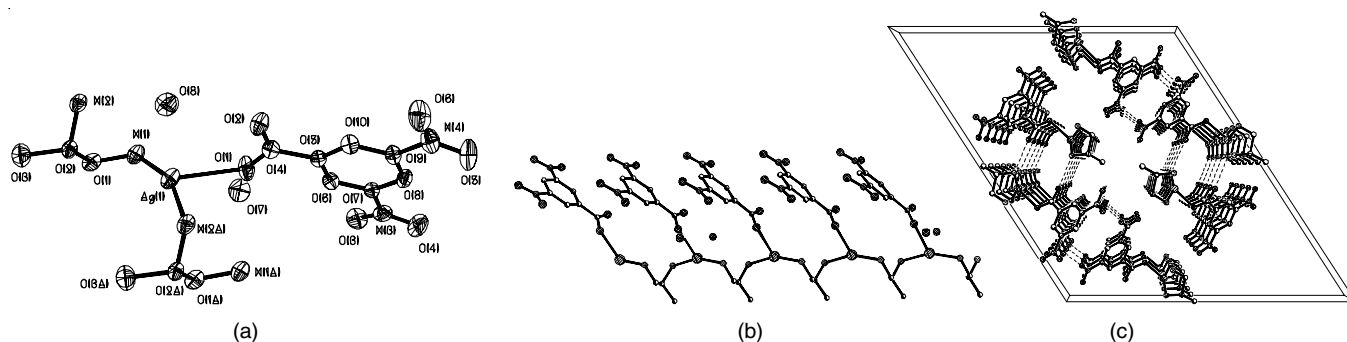


Fig. 1. Coordination environment of Ag(I) ion in **1**(a); Chain-like structure of **1**(b); Perspective view of the stacking array of **1** (c)

Compound **2** crystallizes in triclinic space group P and the asymmetric unit consists of two Ag ions, two dnbc, one ethylenediamine (en) and two crystal lattice water molecules (Fig. 2). The Ag(1) ion has a linear coordination geometry, being coordinated by two nitrogen atoms from two en. The Ag-N distances are 2.149(5) and 2.168(5) Å and the N-Ag-N angle is 175.9(2). The Ag(2) ion also has a linear coordination geometry, being coordinated by two oxygen atoms from two dnbc. The Ag-O distances are 2.147(5) and 2.091(5) Å and the O-Ag-O angle is 174.4(3). Besides, Ag(1) and Ag(2) forms ligand-unsupported Ag...Ag interaction with Ag...Ag distance of 3.177 Å. The en ligands bridge Ag(1) ions to form coordination polymer chain with Ag(dnbc)₂ coordination fragment attached *via* Ag...Ag interaction as shown in Fig. 2b. In addition, there are a variety of O-H...O and C-H...O hydrogen bonds [O(13)...O(14), 2.729; O(13)...O(14), 2.775, O(14)...O(13), 2.775, C(2)...O(7), 2.980, C(7)...O(10), 3.441; C(9)...O(2), 2.826; C(9)...O(13), 3.361; C(14)...O(8), 3.284] which extend the two-dimensional layer into three-dimensional supramolecular array.

Compound **3** crystallizes in triclinic space group P, and the asymmetric unit consists of two Ag ions, two nbc and one en. The Ag(1) ion has a linear coordination geometry, being coordinated by two nitrogen atoms from two en. The Ag-N distances are 2.129(3) and 2.130(3) Å and the N-Ag-N angle is 178.40(12). The Ag(2) ion also has a linear coordination geometry, being coordinated by two oxygen atoms from two dnbc. The Ag-O distances are 2.144(3) and 2.093(3) Å and the O-Ag-O angle is 178.00(11). The Ag(1) and Ag(2) forms ligand-unsupported Ag...Ag interaction with Ag...Ag distance of 3.267 Å. The en ligands link Ag(1) ions to form coordination polymer chain with Ag(nbc)₂ fragments attached *via* Ag...Ag interaction as shown in Fig. 2. In addition, there are a variety of N-H...O and C-H...O hydrogen bonds [N(3)...O(2), 3.063; N(3)...O(6), 3.173; N(4)...O(2), 3.025; N(4)...O(6), 2.950; C(16)...O(1), 3.398] which extend the one-dimensional chain into three-dimensional supramolecular array as shown in Fig. 3.

Compound **4** crystallizes in triclinic space group P, and the asymmetric unit consists of one Ag ions, one dapn, one

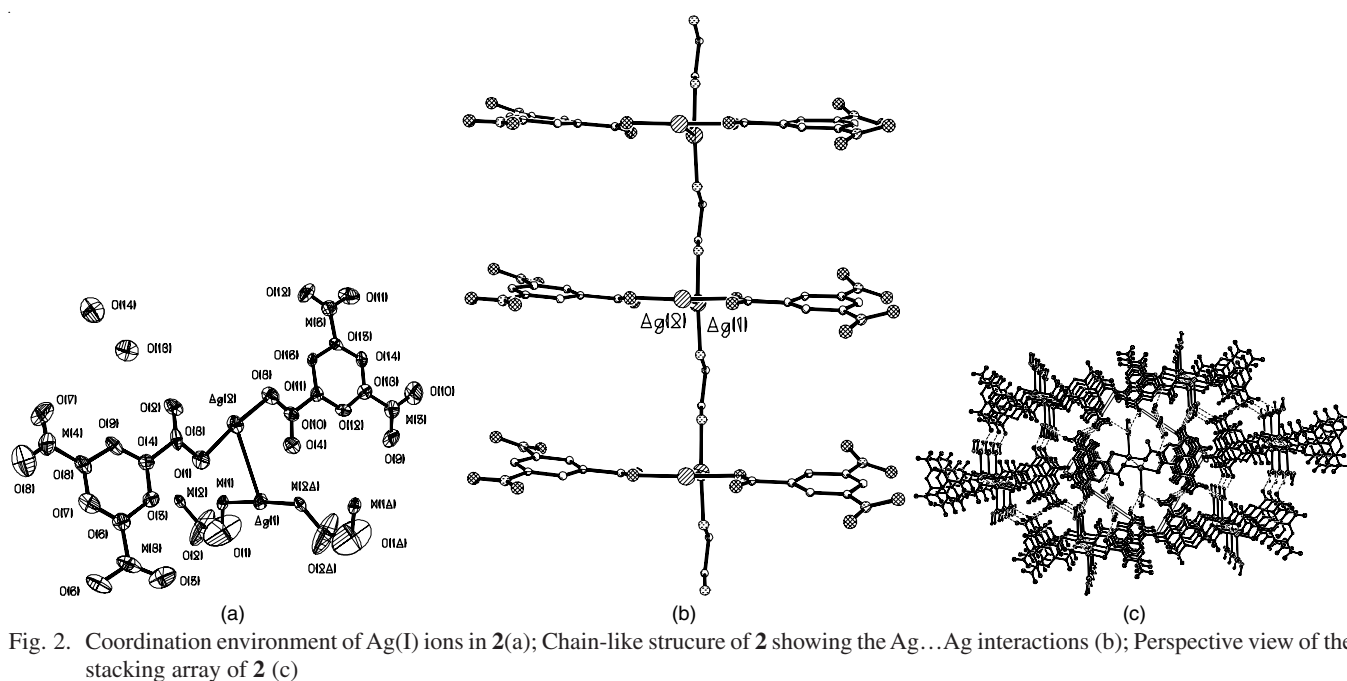


Fig. 2. Coordination environment of Ag(I) ions in **2**(a); Chain-like structure of **2** showing the Ag...Ag interactions (b); Perspective view of the stacking array of **2** (c)

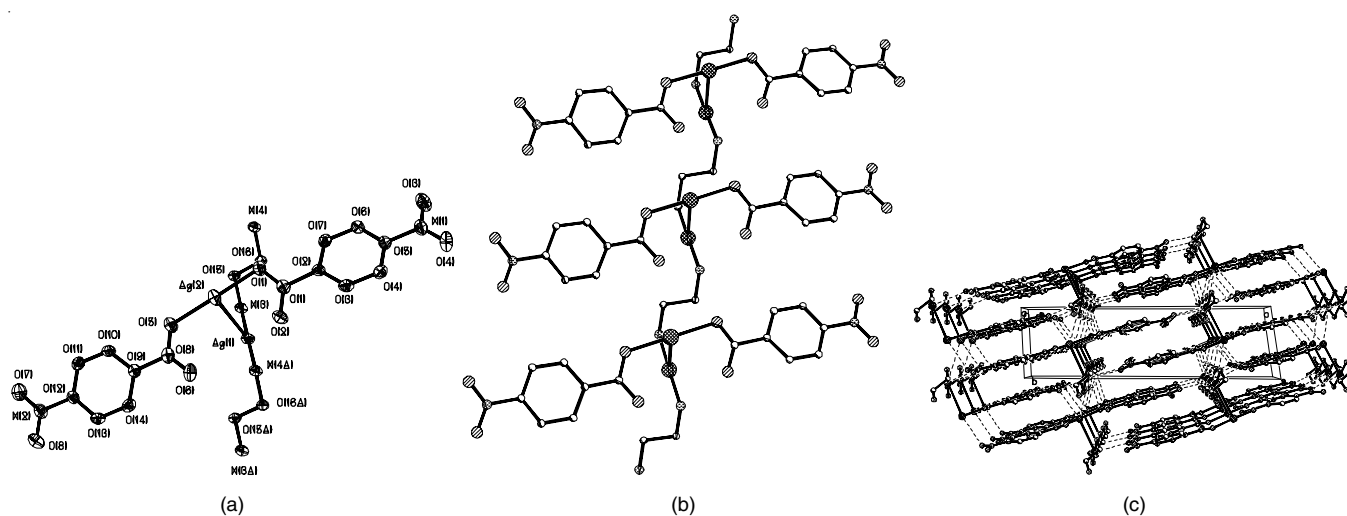


Fig. 3. Coordination environment of Ag(I) ions in **3**(a); Chain-like structure of **3** showing the Ag...Ag interactions (b); Perspective view of the stacking array of **3** (c)

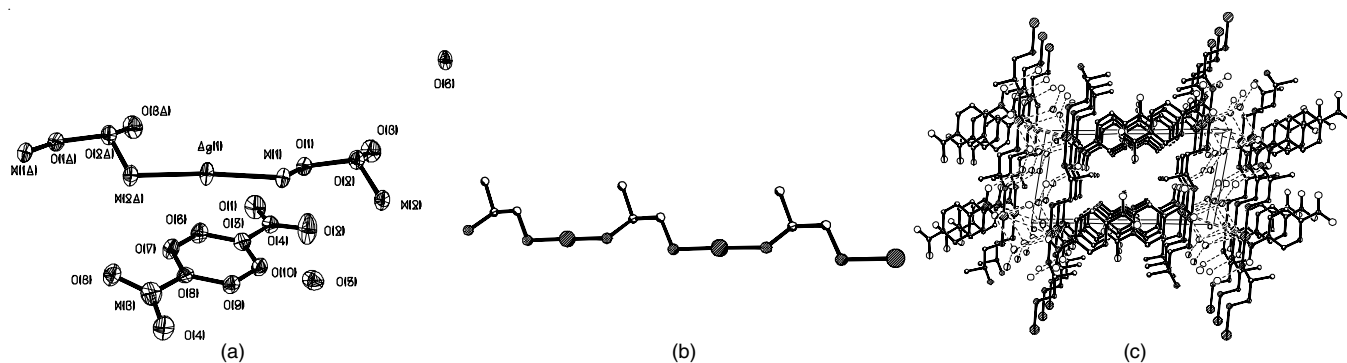


Fig. 4. Coordination environment of Ag(I) ion in 4(a); Chain-like structure of 4 (b); Perspective view of the stacking array of 4 (c)

TABLE-4
CYTOTOXICITIES OF COMPLEXES 1 TO 4

Complex	IC ₅₀ (μM)						
	Hela	HepG2	BGC	95-D	CNE	L-02	NIH3T3
1	5.3	6.2	8.6	7.6	8.4	9.1	4.9
2	4.2	5.9	7.4	4.7	6.2	5.6	12.6
3	6.4	4.3	6.6	4.8	8.3	6.0	4.0
4	8.7	15.4	12.3	21.3	23.8	18.1	6.9

dbc and two crystal lattice water molecules. The Ag(I) ion has a linear coordination geometry, being coordinated by two nitrogen atoms from two dapn. The Ag-N distances are 2.124(3) and 2.132(3) Å and the N-Ag-N angle is 175.50(12). The dbc molecule is pendent and acts as counterion to maintain charge balance. The structure of compound 4 is simple one-dimensional chain constructed from Ag and dmpn ligand. In addition, there are a variety of O-H...O and C-H...O hydrogen bonds [N(1)...O(5), 2.996; N(1)...(6), 3.117; N(2)...O(3), 3.037; N(2)...O(5), 3.020; O(5)...O(3), 2.721; O(5)...O(6), 2.723; O(6)...O(4), 2.722; O(6)...O(4), 2.730; C(7)...O(2), 3.376; C(10)...O(3), 3.348] which extended the two-dimensional layer into three-dimensional supramolecular array as shown in Fig. 4.

Cytotoxicity: The compound concentrations required to yield 50 % inhibition of the viable cells (IC₅₀), determined by the literature method [35] are listed in Table-4. The low IC₅₀ concentrations of these four complexes showed that they are strong cytotoxic *in vitro* [36,37] both to normal cells and carcinoma cells. The high cytotoxicities these compounds imply that these compounds are potential candidates for antitumor agents. On the other hand, different kinds of the cells have different sensitivities to these compounds, therefore, further exploration in generating analogous silver(I) complexes through appropriate chemical modification is required for higher selectivity as well as for understanding the structure function relation.

REFERENCES

- B.J. Hathaway, ed.: G. Wilkinson, Comprehensive Coordination Chemistry, Pergamon: Oxford, vol. 5, pp. 533-591 (1987).
- C.Y. Xu, M.J. Haunden-Smith and T.T. Kodas, Aerosol-Assisted Chemical Vapor Deposition (AACVD) of Binary Alloy (Ag_xPd_{1-x}, Cu_xPd_{1-x}, Ag_xCu_{1-x}) Films and Studies of their Compositional Variation, *Chem. Mater.*, **7**, 1539 (1995); <https://doi.org/10.1021/cm00056a021>.
- M.M.B. Holl, P.F. Seidler, S.P. Kowakzyk and F.R. Mcfeely, Surface Reactivity of Alkylgold(I) Complexes: Substrate-Selective Chemical Vapor Deposition of Gold from RAuP(CH₃)₃ (R = CH₂CH₃, CH₃) at Remarkably Low Temperatures, *Inorg. Chem.*, **33**, 510 (1994); <https://doi.org/10.1021/ic00081a019>.
- J.D. Way and R.D. Noble, ed.: W.S.W. Ho and K.K. Strkar, Facilitated Transport, In: Membrane Handbook, Van Nostrand Reinhold: New York (1992).
- C.D.M. Beverwijk, G.V.D. Kerk, A.J. Leustnk and J.G. Nolter, Organosilver Chemistry, *Organomet. Chem. Rev. A*, **5**, 215 (1970).
- B.C. Gates, Catalytic Chemistry, Wiley: New York, p. 392 (1991).
- R.A. Van Santen and H.P.C.E. Kuipers, The Mechanism of Ethylene Epoxidation, *Adv. Catal.*, **35**, 265 (1987); [https://doi.org/10.1016/S0360-0564\(08\)60095-4](https://doi.org/10.1016/S0360-0564(08)60095-4).
- C.J. Bertole and C.A. Mims, Dynamic Isotope Tracing: Role of Subsurface Oxygen in Ethylene Epoxidation on Silver, *J. Catal.*, **184**, 224 (1999); <https://doi.org/10.1006/jcat.1999.2427>.
- C.-B. Wang, G. Deo and I.E. Wachs, Interaction of Polycrystalline Silver with Oxygen, Water, Carbon Dioxide, Ethylene, and Methanol: In Situ Raman and Catalytic Studies, *J. Phys. Chem. B*, **103**, 5645 (1999); <https://doi.org/10.1021/jp9843631>.
- G. J. Miller, J.B. Metson, G.A. Bowmaker and R.P. Coomey, In situ Raman studies of the selective oxidation of methanol to formaldehyde and ethene to ethylene oxide on a polycrystalline silver catalyst, *J. Chem. Soc., Faraday Trans.*, **91**, 4149 (1995); <https://doi.org/10.1039/FT9959104149>.
- J.K. Plischke, A.J. Benesi and M.A. Vannice, A ¹³C NMR study of ethylene adsorbed on reduced and oxygen-covered ag surfaces, *J. Catal.*, **138**, 223 (1992); [https://doi.org/10.1016/0021-9517\(92\)90019-E](https://doi.org/10.1016/0021-9517(92)90019-E).
- D.J. Sajkowski and M. Boudart, Structure Sensitivity of the Catalytic Oxidation of Ethene by Silver, *Catal. Rev. Sci. Eng.*, **29**, 325 (1987); <https://doi.org/10.1080/01614948708078611>.
- A. Bielanski and J. Haber, Oxygen in Catalysis, Marcel Dekker: New York, p. 279 (1991).
- H.V.R. Dias and Z. Wang, Ethylene Oxide and Propylene Sulfide Complexes of Silver(I): Synthesis and Characterization of [HB(3,5-(CF₃)₂Pz)₃]Ag(OC₂H₄) and [HB(3,5-(CF₃)₂Pz)₃]Ag(SC₃H₆), *Inorg. Chem.*, **39**, 3724 (2000); <https://doi.org/10.1021/ic991334w>.
- I.F. Fieser and M. Fieser, Organic Chemistry, Reinhold: New York, edn 2 (1956).
- A. Yanagisawa, Y. Matsumoto, H. Nakashima, K. Asakawa and H. Yamamoto, Enantioselective Aldol Reaction of Tin Enolates with Aldehydes Catalyzed by BINAP-Silver(I) Complex, *J. Am. Chem. Soc.*, **119**, 9319 (1997); <https://doi.org/10.1021/ja970203w>.

17. A. Yanagisawa, H. Nakashima, A. Ishiba, H. Yamamoto, Catalytic Asymmetric Allylation of Aldehydes Using a Chiral Silver(I) Complex, *J. Am. Chem. Soc.*, **118**, 4723 (1996); <https://doi.org/10.1021/ja9603315>.
18. T. Miyadera, Alumina-supported silver catalysts for the selective reduction of nitric oxide with propene and oxygen-containing organic compounds, *Appl. Catal. B*, **2**, 199 (1993); [https://doi.org/10.1016/0926-3373\(93\)80048-I](https://doi.org/10.1016/0926-3373(93)80048-I).
19. K. Masuda, K. Tsujimura, K. Shinoda and T. Kato, Silver-promoted catalyst for removal of nitrogen oxides from emission of diesel engines, *Appl. Catal. B*, **8**, 33 (1996); [https://doi.org/10.1016/0926-3373\(95\)00051-8](https://doi.org/10.1016/0926-3373(95)00051-8).
20. S. Surniya, H. He, A. Akira, N. Takezawa and K. Yoshida, Formation and Reactivity of Isocyanate (NCO) Species on Ag/Al₂O₃, *J. Chem. Soc., Faraday Trans.*, **94**, 2217 (1998); <https://doi.org/10.1039/A801849I>.
21. F.C. Meunier, J.P. Breen, V. Zuzaniuk, M. Olsson, J.R.H. Ross, Mechanistic Aspects of the Selective Reduction of NO by Propene over Alumina and Silver–Alumina Catalysts, *J. Catal.*, **187**, 493 (1999); <https://doi.org/10.1006/jcat.1999.2622>.
22. H. Deng and P. Kebarle, Binding Energies of Silver Ion–Ligand, L, Complexes AgL²⁺ Determined from Ligand-Exchange Equilibria in the Gas Phase, *J. Phys. Chem. A*, **102**, 571 (1998); <https://doi.org/10.1021/jp973088k>.
23. V. W.-M. Lee, H. Li, T.-C. Lau, K. W. M. Siu, Structures of b and a Product Ions from the Fragmentation of Argentinated Peptides, *J. Am. Chem. Soc.*, **120**, 7302 (1998); <https://doi.org/10.1021/ja9808245>.
24. T. Shoeib, H. El Aribi, K.W.M. Siu and A.C. Hopkinson, A Study of Silver (I) Ion-Organonitrile Complexes: Ion Structures, Binding Energies, and Substituent Effects, *J. Phys. Chem. A*, **105**, 710 (2001); <https://doi.org/10.1021/jp002676m>.
25. R.C. Larock and W.W. Leong, eds.: B.M. Trost and I. Fleming, Comprehensive Organic Synthesis, Pergamon Press: Oxford, U.K., vol. 4, p. 269 (1991).
26. K. Yasutaka, M. Osamu and T. Kazuhide, Stereoselective Addition of Alcohol to Acetylenecarboxylate Catalyzed by Silver(I) Salt, *Chem. Lett.*, **25**, 727 (1996); <https://doi.org/10.1246/cl.1996.727>.
27. H. Veen, Silver thiosulphate: An Experimental Tool in Plant Science, *Sci. Hortic.*, **20**, 211 (1983); [https://doi.org/10.1016/0304-4238\(83\)90001-8](https://doi.org/10.1016/0304-4238(83)90001-8).
28. R.B. Thurman, C.P. Gerba and G. Bitton, The Molecular Mechanisms of Copper and Silver Ion Disinfection of Bacteria and Viruses, *CRC Crit. Rev. Environ. Control*, **18**, 295 (1989); <https://doi.org/10.1080/10643388909388351>.
29. R. Lopez-Gonzalez, G. Alvarez-Cienfuegos, M.A. Romero-Molina, A. Navarrete-Guijosa and M.M. Herrador-Pino, Synthesis, Molecular Structure Determination, and Biological Studies on E-1-p-ethoxyphenyl-4-hydroximinomethyl imidazole Metal Complexes, *J. Inorg. Biochem.*, **38**, 139 (1990); [https://doi.org/10.1016/0162-0134\(90\)84022-H](https://doi.org/10.1016/0162-0134(90)84022-H).
30. K. Nomiya, S. Takahashi, R. Noguchi, S. Nernoto, T. Takayama and M. Oda, Synthesis and characterization of water-soluble silver(I) complexes with L-histidine (H2his) and (S)-(-)-2-pyrrolidone-5-carboxylic acid (H2pyrrld) showing a wide spectrum of effective antibacterial and antifungal activities. Crystal structures of chiral helical polymers [Ag(Hhis)]_n and ([Ag(Hpyrrld)]₂)_n in the solid state, *Inorg. Chem.*, **39**, 3301 (2000); <https://doi.org/10.1021/ic990526o>.
31. F.W. Fuller, M. Parrish and F.C. Nance, A review of the dosimetry of 1% silver sulfadiazine cream in burn wound treatment, *J. Burn Care Rehabil.*, **15**, 213 (1994); <https://doi.org/10.1097/00004630-199405000-00003>.
32. N. Tshipouras, C. J. Rix and P.H. Brady, Passage of silver ions through membrane-mimetic materials, and its relevance to treatment of burn wounds with silver sulfadiazine cream, *Clin. Chem.*, **41**, 87 (1995).
33. C.S. Chu, A. T. McManus, B. A. Jr. Pruitt and A. D. Mason Jr. Therapeutic effects of silver nylon dressings with weak direct current on Pseudomonas aeruginosa-infected burn wounds., *J. Trauma*, **28**, 1488 (1988).
34. G.M. Sheldrick, SHELX-97, Program for Crystal Structure Determination, University of Göttingen: Germany (1997).
35. J. Carmichael, W.C. DeGraff, A.F. Gazdar, J.D. Minna and J.B. Mitchell, Evaluation of a tetrazolium-based semiautomated colorimetric assay: assessment of chemosensitivity testing, *Cancer Res.*, **47**, 936 (1987).
36. B. Rosenberg, L. van Camp, J. E. Trosko and V. H. Mansour, Platinum Compounds: A New Class of Potent Antitumour Agents., *Nature*, **222**, 385(1969); <https://doi.org/10.1038/222385a0>.
37. C.L. Baird, A.E. Griffiths, S. Baffic, P. Bryant, B. Wolf, J. Lutton, M. Berardini and G.M. Arvanitis, Synthesis, characterization and antitumor activity of platinum triamine complexes containing imidazothiazole ligands, *Inorg. Chim. Acta*, **256**, 253(1997); [https://doi.org/10.1016/S0020-1693\(96\)05453-9](https://doi.org/10.1016/S0020-1693(96)05453-9).